
AUDIOFORMER: AUDIO TRANSFORMER LEARNS AUDIO FEATURE REPRESENTATIONS FROM DISCRETE ACOUSTIC CODES

Zhaohui Li^{1,2} Haitao Wang¹ Xinghua Jiang^{1*}

¹YiWise Inc. ²Xidian University

October 11, 2024

ABSTRACT

We propose a method named AudioFormer, which learns audio feature representations through the acquisition of discrete acoustic codes and subsequently fine-tunes them for audio classification tasks. Initially, we introduce a novel perspective by considering the audio classification task as a form of natural language understanding (NLU). Leveraging an existing neural audio codec model, we generate discrete acoustic codes and utilize them to train a masked language model (MLM), thereby obtaining audio feature representations. Furthermore, we pioneer the integration of a **Multi-Positive sample Contrastive** (MPC) learning approach. This method enables the learning of joint representations among multiple discrete acoustic codes within the same audio input. In our experiments, we treat discrete acoustic codes as textual data and train a masked language model using a cloze-like methodology, ultimately deriving high-quality audio representations. Notably, the MPC learning technique effectively captures collaborative representations among distinct positive samples. Our research outcomes demonstrate that AudioFormer attains significantly improved performance compared to prevailing monomodal audio classification models across multiple datasets, and even outperforms audio-visual multimodal classification models on select datasets. Specifically, our approach achieves remarkable results on datasets including AudioSet (2M, 20K), and FSD50K, with performance scores of 53.9, 45.1, and 66, respectively. We have openly shared both the code and models: <https://github.com/LZH-0225/AudioFormer.git>.

1 Introduction

In recent years, alongside the advancement of neural networks, significant breakthroughs have been achieved in audio classification tasks. Currently, three mainstream approaches dominate this field: **1) Convolutional Neural Networks (CNN)-based approaches:** These methods involve designing deeper and wider networks. This category includes methods like DeepResNet [1], TALNet [2], and PANNs [3]. Additionally, strategies such as utilizing pre-training from ImageNet [4], balanced sampling, data augmentation, label augmentation, and model aggregation contribute to enhancing model effectiveness, as demonstrated by PSLA [5]. **2) Transformer-based approaches from the image domain:** such as ViT [7], Swin-Transformer [8], and MAE [9], as backbones. These methods combine various training methodologies to achieve superior outcomes. Examples include AST [10], PaSST [11], HTS-AT [12], and BEATs [13]. These methods not only leverage the backbone's structural advantages but also utilize model parameters pre-trained on the ImageNet [4] dataset. **3) Modal fusion or contrastive learning-based approaches:** drawing insights from audio-text or audio-image multimodal data to enhance monomodal audio capabilities. Methods like MBT [14], UAVM [15], CAV-MAE [16], and MAViL [17] fall under this category. A commonality among these three approaches is that they transform continuous audio signals into Mel Spectrogram through Fourier transformation, treating audio tasks as image-related tasks.

*Corresponding author

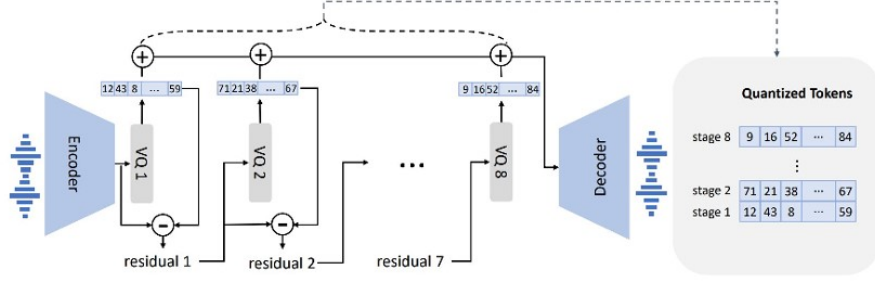


Figure 1: The neural audio codec model revisit. Because RVQ is employed, the first quantizer plays the most important role in reconstruction, and the impact from others gradually decreases, from VALL-E.

In the field of Natural Language Processing (NLP), MLM such as BERT [18], Roberta [19], and RoFormer [20] have achieved groundbreaking results across various NLP tasks by reconstructing masked text tokens on large-scale corpora. The inputs for NLP tasks are inherently discrete signals, which fundamentally differ from the continuous nature of audio signals. In the domain of audio, research based on discrete audio signals has also made significant progress. For example, Hubert [21] treats audio frames as discrete units and employs the MLM approach to learn audio representations. Thanks to advancements in audio compression and Residual Vector Quantization (RVQ) [22,23] technology, breakthroughs like SoundStream [24] and EnCodec [25] utilize RVQ to quantize audio for compression, resulting in improved and faster audio synthesis. VALL-E [26], building upon EnCodec’s discretized audio codes, considers text-to-speech (TTS) as a conditional language modeling task, training a neural codec language model using discrete acoustic codes derived from an off-the-shelf neural audio codec model.

In this study, drawing inspiration from VALL-E, we introduce neural audio codec technology into the domain of audio comprehension tasks, treating audio comprehension as a facet of NLU. Borrowing from the pretraining methods of models like BERT, we delve into the application of reasonable masking rate settings and position encodings to learn audio feature representations from discretized audio acoustic codes. Due to the discrete nature of audio introduced by RVQ technology, distinct stages yield Quantized Tokens (see Figure 1). To enhance the model’s performance in downstream tasks, we have formulated a Multi-Positive sample Contrastive (MPC) learning approach to amalgamate information across different Quantized Tokens (QT). Our approach is referred to as **AudioFormer: Audio Transformer learns audio feature representations from discrete audio codes**.

During the pretraining phase, we discretize continuous audio signals into acoustic codes (Equivalent to QT) using EnCodec. Subsequently, we employ Roformer as the backbone network (utilizing its network structure only, without employing its pretrained model parameters). AudioFormer is pretrained using a 25% masking ratio, following the MLM approach, as illustrated in Figure 2(a).

During the fine-tuning phase, we explored two fine-tuning strategies. **Fine-Tune Method 1**, we removed the MLP layer of the pretrained model and appended a classification head solely for fine-tuning across various downstream tasks, as depicted in Figure 2(b). **Fine-Tune Method 2**, an audio is quantized into multiple acoustic codes, each naturally endowed with multiple positive samples. Inspired by contrastive learning, we introduced a Multi-Positive sample Contrastive (MPC) learning mechanism. Taking the first row of acoustic codes (QT_1) as the anchor, we pulled the remaining rows of codes ($QT_{1\dots N}$) closer to the anchor and pushed away from other audio’s acoustic codes. This approach allows the anchor to learn from the knowledge contained within the other codes while retaining its own capabilities, thereby further enhancing the model’s performance in downstream tasks, as illustrated in Figure 3.

We pre-trained AudioFormer on the AudioSet-2M dataset [27] and fine-tuned it on downstream tasks using AudioSet-2M, AudioSet-20k, and FSD50K [28] datasets. Our approach achieved the state-of-the-art (SOTA) performance in single-modal audio understanding on all four datasets, significantly outperforming previous SOTA results in the audio single-modal domain. Specifically, AudioFormer achieved an mAP (mean Average Precision) of 53.9 on AudioSet-2M, 44.3 on AudioSet-20k, and 65.6 on FSD50K. These results demonstrate that AudioFormer not only outperforms other single-modal audio models on AudioSet-2M and AudioSet-20k but also slightly surpasses the SOTA performance in multi-modal audio-visual results on AudioSet (2M, 20K).

In summary, our contributions are as follows: 1) We introduce AudioFormer, a framework that treats audio understanding tasks as text understanding tasks. In contrast to current mainstream methods that use Mel Spectrogram as inputs,

AudioFormer takes acoustic codes as input. By reconstructing masked tokens, we pre-train the model using a MLM objective. This approach offers a novel direction in the field of audio understanding, while also providing insights for the integration of audio and text in multi-modal tasks. 2) We propose a **Multi-Positive sample Contrastive** (MPC) learning approach, built upon the inherent nature of multiple codes within acoustic codes acting as natural positive instances for one another. Through contrastive learning, this method empowers the anchor to glean knowledge from other positive examples, thus further elevating the model's performance. 3) We achieve single-modal audio SOTA results on various audio understanding benchmarks and slightly surpass or match the current SOTA results in multi-modal audio-visual understanding. We have made our model, code, and discretized audio data open-source to facilitate future research.

2 Related Work

2.1 Models based on Mel Spectrogram

2.1.1 Single-Modal Audio

In the context of CNN-based models. The DeepResNet approach focuses on training a multi-label event classifier directly from audio recordings in AudioSet. The TALNet project concentrates on comparing five different pooling functions and ultimately adopts the linear softmax pooling function. PANNs introduces an architecture called Wavegram-Logmel-CNN, utilizing log-mel spectrograms and waveforms as input features. PSLA proposes the use of an ImageNet supervised pre-trained EfficientNet [29] model for initializing audio models and fine-tuning them on audio classification tasks, resulting in a significant improvement in accuracy.

Models based on the visual Transformer architecture. AST transforms the single-channel Mel Spectrogram into a three-channel representation using a 2D-convolutional layer, with the ViT architecture as its backbone. PaSST's primary contribution involves adding position encodings to both the time and frequency dimensions of the Mel Spectrogram, along with introducing the "patchout" technique to accelerate Transformer model training by reducing sequence length. Its backbone is DeiT B \uparrow 384 [30]. Differing from AST's use of the CLS token for predicting classification labels, HTS-AT takes a distinct approach. HTS-AT contends that this method cannot effectively indicate audio's start and end times similar to CNNs. Therefore, it introduces a Token-semantic CNN layer after the Transformer block, grouping all tokens directly to consider the final output. Its backbone is the Swin-Transformer. SSAST [31] introduces a patch-based self-supervised learning method. It pre-trains the AST using reconstruction and contrastive losses, achieving performance comparable to supervised pre-training.

The Masked Autoencoder (MAE) employs an asymmetric encoder-decoder architecture, where a significant portion of the encoder inputs is masked. A lightweight decoder is trained to reconstruct masked patches based on the unmasked encoded representations, leading to efficient representation learning. Inspired by this, methodologies like MSM-MAE [32], MaskSpec [33], MAE-AST [34], and Audio-MAE [35] apply this approach in the audio domain. While BEATs also utilizes the accelerated training via MAE, it explores a self-supervised audio pre-training method involving masked discrete label prediction objectives. This aspect shares certain similarities with our approach, which we'll detail in section 2.2, discussing the similarities and differences. Another contribution of BEATs is the introduction of an iterative pre-training framework. This involves iteratively training a Tokenizer through distillation to extract more accurate discrete labels. Notably, the backbones used in these aforementioned works are all pre-trained on the ImageNet dataset. In other words, they not only leverage the backbone's model architecture but also its pre-trained parameters.

2.1.2 Multi-Modal

Contrastive learning has been widely utilized to achieve cross-modal alignment in tasks involving image-text and audio-visual domains. Drawing inspiration from the visual pre-training method CLIP [36], CLAP [37] introduces a contrastive language-audio pre-training task, enhancing audio representations through supervised audio-text pairs. CLAR [38] goes beyond using raw waveforms or acoustic features as inputs. Instead, it proposes various data augmentation techniques for both, achieving more effective contrastive learning. Wav2clip [39] takes a different approach by not starting from scratch. It leverages the pre-trained CLIP model and learns additional audio encoders for audio collections through supervised audio and class label pairs.

VATT [40] employs a modality-agnostic single backbone Transformer and shares weights across different modalities. UAVM [15] proposes specific feature extractors and optional modality-specific Transformers for each modality before the shared Transformer. CAV-MAE [16] extends the MAE from single-modal to audio-visual multi-modal scenarios by combining cross-modal contrastive learning and masked data modeling to learn joint audio-visual representations. MAViL [17] not only utilizes MAE and cross-modal contrastive learning but also explores intra-modal contrastive learning and multi-modal masked data reconstruction. Effective contrastive learning is achieved by masking for intra-modal and inter-modal context. For multi-modal MAE, a new proxy task is introduced in MAViL for predicting

aligned and contextualized audio-visual reconstructions, surpassing the performance of reconstructing single-modal raw inputs.

Unlike the use of contrastive learning methods, MBT [14] places a stronger emphasis on modality fusion and introduces a novel architecture based on Transformers. This architecture utilizes "fusion bottlenecks" to compel the bottleneck layers to organize and condense relevant information between each modality.

2.2 Audio Discretization

In recent years, there has been a growing interest in utilizing discrete values to represent various tasks related to audio and speech. Jukebox [41] employs a model based on hierarchical VQ-VAE [42] to learn the audio's discrete representation for music generation tasks. By combining this with an autoregressive model, Jukebox demonstrates the ability to produce high-quality music. On the other hand, HuBERT masks audio frames at the frame level and learns audio representations using a masked language model approach. It employs an iterative hidden state clustering method to generate discrete labels for speech self-supervised learning (SSL) tasks. These hidden states are extracted from the final round of the speech SSL model.

A method similar to ours is BEATs, which is the first to train an acoustic tokenizer under the supervision of the final round of the self-supervised learning (SSL) model. This approach differs from previous autoencoding and temporary clustering methods. It's worth noting that BEATs discretizes labels by calculating distances between Mel Spectrogram blocks and codebooks. However, its input to the Transformer remains the Mel Spectrogram, with a ViT backbone. Essentially, BEATs remains rooted in image tasks.

The aforementioned discretized units following audio discretization are individual distributions, distinct from token-level units in natural language processing. What sets us apart is that we employ a neural audio codec to discretize audio into tokens, which are then inputted into the Transformer. The tokens used in both input and labels remain the same. This approach is entirely consistent with natural language processing tasks.

2.3 Neural Audio Codec

In the past, research on low-bitrate parametric audio and audio codec has been ongoing [43,44], but the quality performance has been unsatisfactory. Despite some progress made [45,46], modeling excitation signals remains a challenging task. Currently, in the realm of traditional audio codecs, Opus [47] and Enhanced Voice Services (EVS) [48] are considered state-of-the-art. These methods not only maintain high encoding efficiency for general audio but also support diverse bit rates, sampling rates, and real-time compression.

With the advancement of neural networks, neural audio codecs [24,25,49,50,51,52,53,54,55,56,57] have demonstrated superior performance compared to traditional methods. Many of these methods involve quantizing the latent space before feeding it to the decoder. The LPCNet [50] vocoder employs handcrafted features and a uniform quantizer as conditions. [58] adjusts WaveNet-based [59] models using discrete units obtained from the VQ-VAE [42] model, while [60] attempts to enhance the perceptual quality of the Opus [48] codec by feeding data into WaveNet. [55,57] propose an autoencoder with a vector quantization layer applied on the latent representation, minimizing reconstruction loss. [56] suggests using Gumbel-Softmax (GS) [61] for representation quantization. SoundStream [24] introduces a fully convolutional encoder-decoder architecture with Residual Vector Quantization (RVQ) [62,63]. The model is optimized using reconstruction loss and adversarial perceptual loss. The EnCodec [25] model inherits RVQ technology and introduces a novel loss balancing mechanism and a lightweight Transformer to further compress the acquired representation by 40%, achieving state-of-the-art results.

3 AudioFormer

3.1 Data Processing

We utilize the pre-trained neural audio codec model, EnCodec [25], as our Tokenizer. Its input and output are variable bitrates 24 kHz audio. The encoder takes in 24 kHz input waveforms and generates embeddings at a rate of 75 Hz, resulting in a downsampled factor of 320. Each embedding is modeled using Residual Vector Quantization (RVQ) [24]. In contrast to VALL-E's [26] choice of 8-level quantizers (see Figure 1), we opt for 4-level quantizers with 1024 entries per quantizer. This setup corresponds to a 3K bitrates for EnCodec. In this configuration, for a given 10-second audio, the discrete representation is a matrix with dimensions of 750×4 , where $750 = \frac{24000 \times 10}{320}$ represents the downsampled time steps, and 4 signifies the number of quantizers.

Given the dataset $D = \{a_i\}$, where a_i represents audio samples, we employ EnCodec to generate acoustic codes denoted as $EnCodec(a) = C^{4*t}$, where C signifies the discrete acoustic encoding matrix, 4 represents acoustic codes comprising 4 rows of acoustic code (designated as C_1, \dots, C_4), and t represents the number of tokens in the acoustic codes after downsampled. After quantization, <BOA> (indicating "begin of audio") is added before the first token of each acoustic code, and <EOA> (indicating "end of audio") is added after the last token.

3.2 Pre-Train

After obtaining the acoustic codes, the goal of AudioFormer during the pre-training phase is to view audio understanding tasks as tasks within the realm of NLP. Leveraging the cloze-style MLM pre-training strategy, AudioFormer aims to acquire robust audio representations for utilization in downstream tasks. In this study, we have opted for RoFormer [20] as our backbone. The rotated position encoding (RoPE) of RoFormer has been demonstrated to excel in learning representations of long texts. It's important to emphasize that we solely utilized its model architecture and did not employ its pre-trained model parameters, (see Figure 2(a)).

Why use RoPE? Due to the fact that a 10-second audio, once quantized into acoustic codes through the neural audio codec, results in a length of 750. AudioFormer faces the challenge of dealing with longer input lengths compared to models like BERT[18], which typically accommodate text sequences of up to 512 tokens. This poses a need for the model to learn contextual information across longer distances. The introduced concept of Rotated Position Embeddings (RoPE) by RoFormer [20] demonstrates superior attenuation capabilities over longer distances, allowing it to better handle extended text data. This is in contrast to BERT's learnable absolute position embeddings and Transformer's sinusoidal position encodings [6]. RoPE exhibits strong performance in flourishing Large Language Models (LLMs) such as GPT-NeoX [64], LLaMA [65] and PaLM [66], showcasing its prowess in handling lengthy textual content.

RoPE is a form of static relative position encoding, serving as a representation of both absolute and relative positional information. It's a method of achieving relative position encoding through the use of absolute position encoding. RoPE adopts an absolute embedding form, yet it manages to capture relative positional relationships.

RoFormer employs RoPE to represent the positions of tokens. The approach involves multiplying the embedding of input x_t at time step t by a rotation matrix $R_{\Theta,t}$.

$$R_{\Theta,t} = \bigoplus_{i=1}^{d/2} M(t, \theta_i) \quad (1)$$

where \oplus represents the direct sum of matrices. d denotes the vector dimension, $i \in [1, 2, \dots, d/2]$. Each $M(t, \theta_i)$ is a 2-D clockwise rotatory matrix of angle $t \cdot \theta_i$.

$$M(t, \theta_i) = \begin{bmatrix} \cos(t \cdot \theta_i) & \sin(t \cdot \theta_i) \\ -\sin(t \cdot \theta_i) & \cos(t \cdot \theta_i) \end{bmatrix} \quad (2)$$

RoPE distorts the embedding space, such that the attention between a token at position m and a token at position n linearly depends on $m - n$. In other words, the attention scores (q_m, k_n) are solely determined by the relative positional offset between them. It modifies the standard attention calculation for attention scores.

$$q_m k_n^T = (x_m W^Q) R_{\Theta, n-m} (x_n W^K)^T \quad (3)$$

Where x_m, x_n are the embeddings at positions m and n , respectively, W_q, W_k represent the query and key weights, and T denotes the transpose.

Why choose a 25% masking rate? Regarding the learning of discrete audio representations, we employ a masked language model that utilizes the cloze-style approach to learn audio feature representations. This approach was introduced by BERT and has achieved significant success in the field of natural language understanding. However, unlike tightly packed information within natural language sentences, in the process of audio discretization through EnCodec, due to the sliding window concept and the redundancy inherent in audio content, the discretized information becomes sparser compared to text. This phenomenon is manifested in the data as:

$$[\dots, 475, 106, 738, 408, \dots, 738, 738, 738, \dots, 133, 133, \dots, 876, 876, \dots, 855, 855, \dots] \quad (4)$$

As evident from the specific data, it contains a substantial number of consecutive identical tokens. This phenomenon results in a decrease in the model's learning difficulty if a lower masking rate is chosen. Therefore, we slightly increase the masking rate to train the model and obtain better representations. Regarding the performance of models with different masking rates.

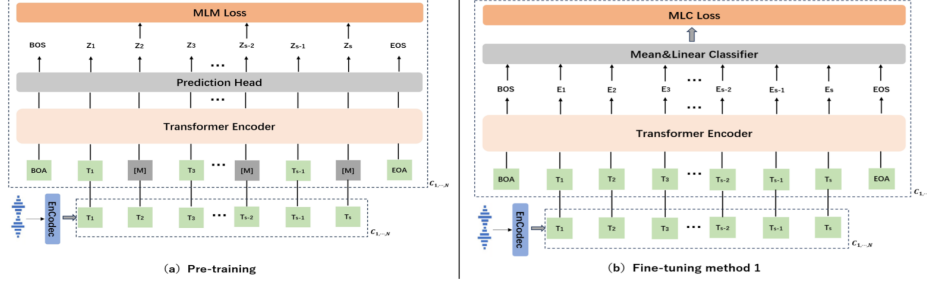


Figure 2: (a).Pre-Train.(b).Fine-Tune method 1

3.3 Fine-Tune

During the fine-tuning phase, AudioFormer employs two distinct strategies for downstream task adaptation. **Fine-Tune Method 1**, the MLP layers excluding the MLM are removed after pretraining, and a separate classification head is added, as shown in Figure 2(b). **Fine-Tune Method 2** introduces a technique termed "Multi-Positive sample Contrastive Learning". Audio is quantized into acoustic codes (C^{4*t}). The first acoustic code (C_1) holds the richest information, while $C_2 \dots C_4$ progressively carry decreasing information with varying emphasis. Inspired by contrastive learning, with C_1 as the anchor, $C_2 \dots C_4$ as its positive examples, and acoustic codes from other audios in the same batch as negatives, we propose the **Multi-Positive sampel Contrastive Learning (MPC)** method. This facilitates the anchor in assimilating the knowledge of the other codes, enhancing AudioFormer's performance in downstream tasks.

3.3.1 Fine-Tune method 1 (FT₁)

Classification tasks are commonly divided into multi-class tasks and multi-label tasks. For multi-class tasks, the cross-entropy (CE) function is commonly used as the loss function. In contrast, for multi-label classification tasks, the binary cross-entropy (BCE) loss is typically employed. Essentially, the BCE loss transforms the multi-label classification task into a set of multiple binary classification tasks.

$$l_{ce} = -\log \frac{e^i}{\sum_{j=1}^{L_{all}} e^j} = \log \left(1 + \sum_{j=1, j \neq i}^{L_{all}} e^{j-i} \right) \quad (5)$$

$$l_{bce} = \sum_{j \in L_{all}, \notin L_g} \log (1 + e^j) + \sum_{i \in L_g} \log (1 + e^{-i}) \quad (6)$$

Eq.5 and Eq.6 respectively represent the computation of individual sample losses for multi-class and multi-label classification tasks. In these equations, i signifies the true class, j denotes all classes or non-true classes, L_{all} signifies the total number of classes, and L_g represents the number of true classes.

For the downstream task of AudioSet, which involves multi-label classification, the task exhibits a significant class imbalance issue due to the fact that $L_{all}(527) \gg L_g(< 10)$. This unbalance poses a challenge. In contrast to the "softmax + cross-entropy" approach commonly used in multi-class tasks, which to a certain extent alleviates class unbalance, we have adopted the LSEP Loss [67] method. This method extends "softmax + cross-entropy" to the context of multi-label classification tasks. It mitigates the class unbalance issue by leveraging the well-balanced properties of the log-sum-exp operation, which automatically balances the weights for each element.

$$l_{LSEP} = \log \left(1 + \sum_{j \in L_{all}, \notin L_g} e^j \sum_{i \in L_g} e^{-i} \right) \quad (7)$$

Eq.7 is also Eq.1 in Circle Loss[68].

3.3.2 Fine-Tune method 2 (FT₂)

As shown in Figure 3, FT₂ adopts a multi-task learning approach for fine-tuning downstream tasks. Our first task involves the fine-tuning method mentioned in FT₁. For the second task, inspired by contrastive learning, LESP Loss [67] and Circle Loss [68], we design a loss function for Multi-Positive sample Contrastive learning (MPC Loss). Specifically, we use the pre-trained model of C_1 as the anchor model, while the pre-trained models of $C_2 \dots C_4$ (with

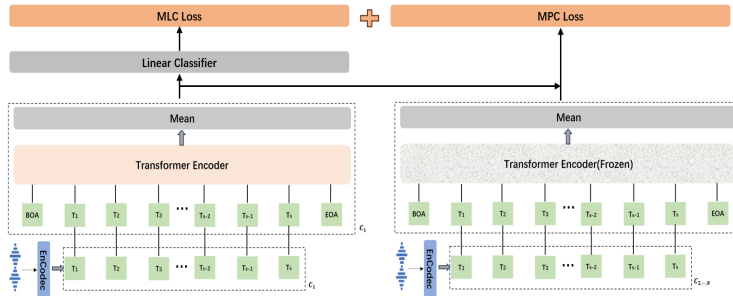


Figure 3: Fine-Tune method 2

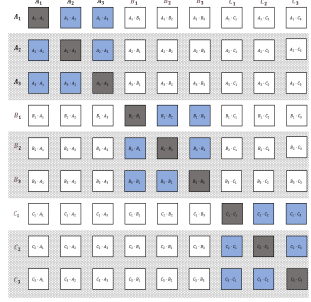


Figure 4: MPC: A, B, and C represent audio samples in the batch. 1, 2, 3 represent quantized acoustic codes. The shaded part indicates exclusion from computation.

frozen parameters) provide positive samples. The purpose of the first task is to ensure the anchor model's competency in downstream tasks. In the second task, by bringing positive samples closer and pushing away negative samples, we integrate the knowledge from the corresponding $C_2 \cdots C_4$ models into the anchor model, thus enhancing performance in downstream tasks.

According to the analysis of EnCodec [25] in VALL-E [26] (refer to Figure 1), the importance of $C_1 \dots C_4$ progressively decreases. Therefore, we choose the model corresponding to C_1 as the anchor. We consider MPC learning as a form of model ensemble that does not increase the parameter count, differing from traditional ensemble methods where increased capacity comes with the cumulative parameters of multiple models. In FT₂, only the anchor model is trained, while the parameters of the remaining $C_2 \dots C_4$ models are frozen. Consequently, this training incurs only a marginal time cost increase. During inference, we discard the $C_2 \dots C_4$ models and utilize C_1 as input for the anchor model. This approach maintains the parameter count identical to FT₁. In conclusion, MPC learning enhances model performance with a negligible increase in training and inference costs.

MPC Loss. For ease of explanation, we'll illustrate with B (batch size) and N ($C_1 \cdots C_3$) both set to 3. First, we construct positive and negative pairs. The positive examples for each acoustic code consist of the other acoustic codes from the same audio. The negative examples involve all acoustic codes from other audios within the same batch. Next, we compute the cosine similarity between the feature representations of all acoustic code pairs in the $B * N$ set. This similarity matrix takes the form shown in Figure 4, where we mask the diagonal as it represents the self-similarity. Since the parameters of models corresponding to $C_1 \cdots C_2$ remain unchanged, we solely compute the MPC Loss for anchor-related samples.

$$MPC_{Loss} = \log(1 + \sum_{a=1, a \neq \Delta}^B \sum_{c=1}^N e^{sim(\Delta_1, a_c) / \tau} \sum_{c=2}^N -e^{sim(\Delta_1, \Delta_c) / \tau}) \quad (8)$$

Where, B represents batch size, N represents the number of acoustic code, Δ represents the acoustic code for which the loss is being computed, a represents other audio samples in the batch, c represents specific entries of acoustic codes, sim represents calculating cosine similarity, and τ represents the temperature parameter in contrastive learning.

The complete loss function for FT_2 is as follows:

$$l = \alpha MLC_{Loos} + (1 - \alpha) MPC_{Loos} \quad (9)$$

Where, α is a hyperparameter, MLC stands for the loss function of Multi-Label Classification

4 Experiments

4.1 Datasets

We pre-trained AudioFormer on the AudioSet-2M dataset and evaluated it on four downstream tasks: three multi-label classification tasks (AudioSet-2M, AudioSet-20k, FSD50K)

AudioSet (AudioSet-2M and AudioSet-20k) is an audio event dataset comprising over two million manually annotated 10-second video clips. These clips are sourced from YouTube, resulting in instances of varying quality and containing

multiple audio sources. The dataset is labeled with 527 audio event classes, with each clip potentially annotated with multiple audio event classes. It is formally divided into three partitions: the balanced set (22,176 clips), the unbalanced set (2,042,985 clips), and the evaluation set (20,383 clips). Due to the dynamic nature of YouTube video availability, which includes cases like video deletions or takedowns, we have downloaded and processed 20,550, 1,932,574, and 18,886 clips for the balanced, unbalanced, and evaluation sets, respectively.

During the pre-training phase, we conducted pre-training using a combination of the balanced and unbalanced datasets. In the fine-tuning phase, for the AS-2M task, we fine-tuned the audio using a combination of the balanced dataset and the 1.9M unbalanced dataset. For the AS-20K task, we solely employed the balanced dataset for fine-tuning. We utilized the mean Average Precision (mAP) evaluation metric to assess the performance of our model on the 19K evaluation set.

Freesound Database 50K (FSD50K) is an open dataset containing 51,197 Freesound clips, which are unevenly distributed among 200 categories in the AudioSet. FSD50K is created by the Music Technology Group at Pompeu Fabra University. It primarily consists of sound events generated by physical sources and production mechanisms. These encompass human sounds, environmental sounds, animal sounds, natural sounds, instrument sounds, and more.

4.2 Implementation Details

Backbone AudoFormer consists of 12 layers of Transformer encoder, each with 768-dimensional hidden states and 12 attention heads. Due to the acoustic code values ranging from [0, 1023], we introduce special tokens <BOA>, <EOA>, <PAD>, and <MASK>, corresponding to token IDs 0, 2, 1, and 1027, respectively. This expands the value range to [0, 1027]. As a result, the dimensions of the embedding layer and the pre-trained model MLP become 1028-dimensional, leading to a model parameter count of 87M.

Pre-Train We resampled the audio data to 24 kHz and used a bitrate of 3 kbps to obtain acoustic codes for EnCodec, resulting in a total of 4 acoustic codes. We applied a MLM pre-training approach to $C_1 \dots C_4$ with a masking rate of 25% for each. Each model was trained for 10 epochs with a learning rate of 1e-4. We compared the performance of models trained on different acoustic code configurations in downstream task fine-tuning. Additionally, we examined the impact of varying masking rates on pre-trained models to validate the appropriateness of the masking rate settings.

Fine-Tune We removed the pre-trained MLP layer while retaining the backbone. In contrast to the common practice in text tasks of using the <CLS> token’s vector for downstream task fine-tuning, we took a different approach. We averaged the model outputs corresponding to all tokens and used this average for fine-tuning in downstream tasks. AudioFormer was exclusively pre-trained on AudioSet-2M. We fine-tuned it on various downstream audio classification datasets of different scales and compared it against other models.

FT₁ For AudioSet-20k, we set the learning rate to 1e-4, trained for 10 epochs, and employed early stopping. Regarding AudioSet-2M, we followed a similar approach to previous research. We initially performed weighted sampling on the unbalanced data. We conducted fine-tuning for 1 epoch on the sampled data using a learning rate of 1e-4. Subsequently, we fine-tuned for 10 epochs on the balanced data with a learning rate of 1e-5, also implementing early stopping. Notably, unlike prior methodologies, we abstained from using deep learning techniques such as warm-up, mixup, data augmentation, and similar tricks.

In the earlier sections, we primarily focused on AudioSet. To assess the general applicability of the proposed AudioFormer technique, we conducted a separate set of experiments on the FSD50K datasets. Specifically, we performed experiments on FSD50K by fine-tuning models that were loaded with pre-trained weights and models fine-tuned on AudioSet.

For the FSD50K dataset, given the variable audio lengths, we applied either padding or truncation to standardize them to 10 seconds. For models loaded with pre-trained weights and subsequently fine-tuned, we set the learning rate to 1e-4, conducted training for 10 epochs, and implemented early stopping. Similarly, for models fine-tuned on AudioSet and then loaded, we used a learning rate of 1e-4, trained for 10 epochs, and employed early stopping.

FT₂ In order to demonstrate the effectiveness of our proposed multi-positive sample contrastive learning, we kept all training parameters consistent with FT1, except for the parameters required for contrastive learning τ and multi-task learning α . We conducted comparisons on AudioSet-2M, AudioSet-20k, and FSD50K to evaluate the impact of varying numbers of positive samples. Due to the phased Fine-Tuning on AudioSet-2M, we did not contrast the effects of the second phase (FT2). We set the value of α to 0.95 for multi-task learning. For the parameter τ , we adhered to the common contrastive learning setting of 0.05.

Overall, AudioFormer achieves state-of-the-art performance in all four audio classification tasks when considered as a single modality. AudioFormer FT1 and FT2 set new benchmarks for single-modality audio understanding performance on AudioSet-2M and AudioSet-20k datasets, surpassing not only previous single-modality speech SOTA results but

Table 1: Comparison of Single-Modal and Multi-Modal Models for Audio Classification. IN, AS, and LS represent ImageNet, AudioSet, and LibraSpeech datasets, respectively. The evaluation indicator is mAP, * indicating the loaded Fine-tune model in AS-2M rather than the pre-trained model

Model	Data	AS-20k	AS-2M*	AS-2M	FSD50K
Single-Modal Audio					
PANN	AS	27.8	-	43.1	-
PSLA	IN	31.9	-	44.4	56.71
PaSST	IN+AS	-	-	47.1	65.55
HTS-AT	IN+AS	-	-	47.1	-
AST	IN+AS	-	-	45.9	-
Audio-MAE	AS	37.1	-	47.3	-
Audio-MAE Large	AS	37.6	-	47.4	-
SS-SAT	AS+LS	31.0	-	-	-
MSM-MAE	AS	-	-	-	-
MaskSpec	AS	32.3	-	47.1	-
MAE-AST	AS+LS	30.6	-	-	-
BEATs	AS	38.9	-	48.6	-
Multi-Modal					
MBT	IN-21K	-	-	49.6	-
UAVM	AS+IN	-	-	-	-
CAV-MAE	AS+IN	42.0	-	51.2	-
MAViL	AS+IN	44.9	-	53.3	-
OURS					
FT ₁	AS	44.6	49.7	53.9	61.5
FT ₂	AS	45.1	50.0	-	62.0
FT ₁ *	AS	-	-	-	65.6

also outperforming multi-modal SOTA results. For instance, on AudioSet-2M, the performance is as follows: for single modality, it achieves 53.9 compared to the previous 48.6, and for multi-modal, it reaches 53.9 compared to 53.3. Similarly, on AudioSet-20k, it scores 45.1 as a single modality compared to 38.9 previously, and in the multi-modal case, it reaches 45.1 compared to 44.9.

It's noteworthy that AudioFormer is only pre-trained on AudioSet-2M but still performs significantly better on other downstream tasks compared to models that were pre-trained using more domain-specific or domain-agnostic data in a supervised or self-supervised manner.

5 Conclusion

In this paper, we introduce AudioFormer, which learns audio feature representations from discrete acoustic codes. Unlike the current mainstream models that use Mel Spectrogram as input, we employ discrete acoustic codes as input and apply techniques from NLP to address audio classification tasks. Given that acoustic codes can vary, we propose a Multi-Positive sample Contrastive learning approach to bring closer different acoustic code from the same audio while pushing away acoustic codes from other audio samples. This strategy enhances performance in downstream tasks and can be seen as a parameter-consistent model ensemble. AudioFormer achieves SOTA results in three audio classification tasks and significantly outperforms the single-modality SOTA performance on the AudioSet (2M, 20K) dataset. It even surpasses the performance of SOTA models designed for audio-visual multi-modality tasks. The remarkable performance in downstream tasks validates the effectiveness of AudioFormer.

The breakthroughs in Large Language Models (LLMs) inspire us greatly. Moving forward, we aspire to explore more possibilities with AudioFormer, extending beyond the boundaries of audio classification tasks. Simultaneously, we provide novel insights for speech-text multi-modal tasks as well.

References

- [1] F. Huang, J. Ash, J. Langford, et al. Learning deep ResNet blocks sequentially using boosting theory. In *International Conference on Machine Learning*, PMLR, 2018, pp. 2058-2067.
- [2] J. X. Zhang, K. Richmond, Z. H. Ling, et al. Talnet: Voice reconstruction from tongue and lip articulation with transfer learning from text-to-speech synthesis. In *Proceedings of the AAAI Conference on Artificial Intelligence*, vol. 35, no. 16, 2021, pp. 14402-14410.
- [3] Q. Kong, Y. Cao, T. Iqbal, et al. Panns: Large-scale pretrained audio neural networks for audio pattern recognition. *IEEE/ACM Transactions on Audio, Speech, and Language Processing*, vol. 28, 2020, pp. 2880-2894.
- [4] A. Krizhevsky, I. Sutskever, and G. E. Hinton. Imagenet classification with deep convolutional neural networks. *Advances in neural information processing systems*, vol. 25, 2012.
- [5] Y. Gong, Y. A. Chung, and J. Glass. Psla: Improving audio tagging with pretraining, sampling, labeling, and aggregation. *IEEE/ACM Transactions on Audio, Speech, and Language Processing*, vol. 29, 2021, pp. 3292-3306.
- [6] A. Vaswani, N. Shazeer, N. Parmar, et al. Attention is all you need. *Advances in neural information processing systems*, vol. 30, 2017.
- [7] A. Dosovitskiy, L. Beyer, A. Kolesnikov, et al. An image is worth 16x16 words: Transformers for image recognition at scale. *arXiv preprint arXiv:2010.11929*, 2020.
- [8] Z. Liu, Y. Lin, Y. Cao, et al. Swin transformer: Hierarchical vision transformer using shifted windows. In *Proceedings of the IEEE/CVF International Conference on Computer Vision*, 2021, pp. 10012-10022.
- [9] K. He, X. Chen, S. Xie, et al. Masked autoencoders are scalable vision learners. In *Proceedings of the IEEE/CVF Conference on Computer Vision and Pattern Recognition*, 2022, pp. 16000-16009.
- [10] Y. Gong, Y. A. Chung, and J. Glass. AST: Audio spectrogram transformer. *arXiv preprint arXiv:2104.01778*, 2021.
- [11] K. Koutini, J. Schlueter, H. Eghbal-Zadeh, et al. Efficient training of audio transformers with patchout. *arXiv preprint arXiv:2110.05069*, 2021.
- [12] K. Chen, X. Du, B. Zhu, et al. HTS-AT: A hierarchical token-semantic audio transformer for sound classification and detection. In *ICASSP 2022 - 2022 IEEE International Conference on Acoustics, Speech and Signal Processing (ICASSP)*, IEEE, 2022, pp. 646-650.
- [13] S. Chen, Y. Wu, C. Wang, et al. Beats: Audio pre-training with acoustic tokenizers. *arXiv preprint arXiv:2212.09058*, 2022.
- [14] A. Nagrani, S. Yang, A. Arnab, et al. Attention bottlenecks for multimodal fusion. *Advances in Neural Information Processing Systems*, vol. 34, 2021, pp. 14200-14213.
- [15] Y. Gong, A. H. Liu, A. Rouditchenko, et al. UAVm: Towards unifying audio and visual models. *IEEE Signal Processing Letters*, vol. 29, 2022, pp. 2437-2441.
- [16] Y. Gong, A. Rouditchenko, A. H. Liu, et al. Contrastive audio-visual masked autoencoder. In *The Eleventh International Conference on Learning Representations*, 2022.
- [17] P. Y. Huang, V. Sharma, H. Xu, et al. MAViL: Masked Audio-Video Learners. *arXiv preprint arXiv:2212.08071*, 2022.
- [18] J. Devlin, M. W. Chang, K. Lee, et al. BERT: Pre-training of deep bidirectional transformers for language understanding. *arXiv preprint arXiv:1810.04805*, 2018.
- [19] Y. Liu, M. Ott, N. Goyal, et al. RoBERTa: A robustly optimized BERT pretraining approach. *arXiv preprint arXiv:1907.11692*, 2019.
- [20] J. Su, Y. Lu, S. Pan, et al. RoFormer: Enhanced transformer with rotary position embedding. *arXiv preprint arXiv:2104.09864*, 2021.
- [21] W. N. Hsu, B. Bolte, Y. H. H. Tsai, et al. Hubert: Self-supervised speech representation learning by masked prediction of hidden units. *IEEE/ACM Transactions on Audio, Speech, and Language Processing*, vol. 29, 2021, pp. 3451-3460.
- [22] A. Gersho and R. M. Gray. Vector quantization and signal compression. *Springer Science & Business Media*, 2012.
- [23] A. Vasuki and P. T. Vanathi. A review of vector quantization techniques. *IEEE Potentials*, vol. 25, no. 4, 2006, pp. 39-47.

[24] N. Zeghidour, A. Luebs, A. Omran, et al. Soundstream: An end-to-end neural audio codec. *IEEE/ACM Transactions on Audio, Speech, and Language Processing*, vol. 30, 2021, pp. 495-507.

[25] A. Défossez, J. Copet, G. Synnaeve, et al. High fidelity neural audio compression. *arXiv preprint arXiv:2210.13438*, 2022.

[26] C. Wang, S. Chen, Y. Wu, et al. Neural Codec Language Models Are Zero-Shot Text to Speech Synthesizers, 2023. URL: <https://arxiv.org/abs/2301.02111>. doi: 10.

[27] J. F. Gemmeke, D. P. W. Ellis, D. Freedman, et al. Audio set: An ontology and human-labeled dataset for audio events. In *2017 IEEE International Conference on Acoustics, Speech and Signal Processing (ICASSP)*, IEEE, 2017, pp. 776-780.

[28] E. Fonseca, X. Favery, J. Pons, et al. FSD50K: An open dataset of human-labeled sound events. *IEEE/ACM Transactions on Audio, Speech, and Language Processing*, vol. 30, 2021, pp. 829-852.

[29] B. Koonce and B. Koonce. EfficientNet. *Convolutional Neural Networks with Swift for TensorFlow: Image Recognition and Dataset Categorization*, 2021, pp. 109-123.

[30] H. Touvron, M. Cord, M. Douze, et al. Training data-efficient image transformers & distillation through attention. In *International Conference on Machine Learning*, PMLR, 2021, pp. 10347-10357.

[31] Y. Gong, C. I. Lai, Y. A. Chung, et al. SSAST: Self-supervised audio spectrogram transformer. In *Proceedings of the AAAI Conference on Artificial Intelligence*, vol. 36, no. 10, 2022, pp. 10699-10709.

[32] D. Niizumi, D. Takeuchi, Y. Ohishi, et al. Masked spectrogram modeling using masked autoencoders for learning general-purpose audio representation. In *HEAR: Holistic Evaluation of Audio Representations*, PMLR, 2022, pp. 1-24.

[33] D. Chong, H. Wang, P. Zhou, et al. Masked spectrogram prediction for self-supervised audio pre-training. In *ICASSP 2023 - 2023 IEEE International Conference on Acoustics, Speech and Signal Processing (ICASSP)*, IEEE, 2023, pp. 1-5.

[34] A. Baade, P. Peng, D. Harwath. MAE-AST: Masked autoencoding audio spectrogram transformer. *arXiv preprint arXiv:2203.16691*, 2022.

[35] P. Y. Huang, H. Xu, J. Li, et al. Masked autoencoders that listen. *arXiv preprint arXiv:2207.06405*, 2022.

[36] A. Radford, J. W. Kim, C. Hallacy, et al. Learning transferable visual models from natural language supervision. In *International Conference on Machine Learning*, PMLR, 2021, pp. 8748-8763.

[37] J. Huang, C. Zhang, J. Dolby. CLAP: Recording local executions to reproduce concurrency failures. *ACM SIGPLAN Notices*, vol. 48, no. 6, 2013, pp. 141-152.

[38] H. Al-Tahan and Y. Mohsenzadeh. CLAR: Contrastive learning of auditory representations. In *International Conference on Artificial Intelligence and Statistics*, PMLR, 2021, pp. 2530-2538.

[39] H. H. Wu, P. Seetharaman, K. Kumar, et al. Wav2clip: Learning robust audio representations from clip. In *ICASSP 2022 - 2022 IEEE International Conference on Acoustics, Speech and Signal Processing (ICASSP)*, IEEE, 2022, pp. 4563-4567.

[40] H. Akbari, L. Yuan, R. Qian, et al. VATT: Transformers for multimodal self-supervised learning from raw video, audio and text. In *Advances in Neural Information Processing Systems*, vol. 34, 2021, pp. 24206-24221.

[41] P. Dhariwal, H. Jun, C. Payne, et al. Jukebox: A generative model for music. *arXiv preprint arXiv:2005.00341*, 2020.

[42] A. Van Den Oord, O. Vinyals. Neural discrete representation learning. In *Advances in Neural Information Processing Systems*, vol. 30, 2017.

[43] B. S. Atal, S. L. Hanauer. Speech analysis and synthesis by linear prediction of the speech wave. *The Journal of the Acoustical Society of America*, vol. 50, no. 2B, 1971, pp. 637-655.

[44] B. H. Juang, A. Gray. Multiple stage vector quantization for speech coding. In *ICASSP'82 - IEEE International Conference on Acoustics, Speech, and Signal Processing*, IEEE, 1982, pp. 597-600.

[45] D. Griffin, J. Lim. A new model-based speech analysis/synthesis system. In *ICASSP'85 - IEEE International Conference on Acoustics, Speech, and Signal Processing*, IEEE, 1985, pp. 513-516.

[46] A. McCree, K. Truong, E. B. George, et al. A 2.4 kbit/s MELP coder candidate for the new US Federal Standard. In *1996 IEEE International Conference on Acoustics, Speech, and Signal Processing Conference Proceedings*, IEEE, 1996, pp. 200-203.

[47] J. M. Valin, V. Eksler, T. Terriberry. Definition of the Opus audio codec. *Xiph.Org*, 2012.

[48] M. Dietz, M. Multrus, V. Eksler, et al. Overview of the EVS codec architecture. In *2015 IEEE International Conference on Acoustics, Speech and Signal Processing (ICASSP)*, IEEE, 2015, pp. 5698-5702.

[49] W. B. Kleijn, F. S. C. Lim, A. Luebs, et al. Wavenet based low rate speech coding. In *2018 IEEE International Conference on Acoustics, Speech and Signal Processing (ICASSP)*, IEEE, 2018, pp. 676-680.

[50] J. M. Valin, J. Skoglund. A real-time wideband neural vocoder at 1.6 kb/s using LPCNet. *arXiv preprint arXiv:1903.12087*, 2019.

[51] F. S. C. Lim, W. B. Kleijn, M. Chinen, et al. Robust low rate speech coding based on cloned networks and wavenet. In *ICASSP 2020 - 2020 IEEE International Conference on Acoustics, Speech and Signal Processing (ICASSP)*, IEEE, 2020, pp. 6769-6773.

[52] W. B. Kleijn, A. Storus, M. Chinen, et al. Generative speech coding with predictive variance regularization. In *ICASSP 2021 - 2021 IEEE International Conference on Acoustics, Speech and Signal Processing (ICASSP)*, IEEE, 2021, pp. 6478-6482.

[53] A. Omran, N. Zeghidour, Z. Borsos, et al. Disentangling speech from surroundings with neural embeddings. *arXiv preprint arXiv:2203.15578*, 2022.

[54] J. Lin, K. Kalgaonkar, Q. He, et al. Speech enhancement for low bit rate speech codec. In *ICASSP 2022 - 2022 IEEE International Conference on Acoustics, Speech and Signal Processing (ICASSP)*, IEEE, 2022, pp. 7777-7781.

[55] T. Jayashankar, T. Koehler, K. Kalgaonkar, et al. Architecture for variable bitrate neural speech codec with configurable computation complexity. In *ICASSP 2022 - 2022 IEEE International Conference on Acoustics, Speech and Signal Processing (ICASSP)*, IEEE, 2022, pp. 861-865.

[56] S. Li, H. H. Mao, J. McAuley. Variable bitrate discrete neural representations via causal self-attention. In *2nd Pre-registration Workshop (NeurIPS 2021), Remote*.

[57] X. Jiang, X. Peng, C. Zheng, et al. End-to-end neural speech coding for real-time communications. In *ICASSP 2022 - 2022 IEEE International Conference on Acoustics, Speech and Signal Processing (ICASSP)*, IEEE, 2022, pp. 866-870.

[58] C. Gârbacea, A. van den Oord, Y. Li, et al. Low bit-rate speech coding with VQ-VAE and a WaveNet decoder. In *ICASSP 2019 - 2019 IEEE International Conference on Acoustics, Speech and Signal Processing (ICASSP)*, IEEE, 2019, pp. 735-739.

[59] A. Oord, S. Dieleman, H. Zen, et al. Wavenet: A generative model for raw audio. *arXiv preprint arXiv:1609.03499*, 2016.

[60] J. Skoglund, J. M. Valin. Improving Opus low bit rate quality with neural speech synthesis. *arXiv preprint arXiv:1905.04628*, 2019.

[61] E. Jang, S. Gu, B. Poole. Categorical reparameterization with gumbel-softmax. *arXiv preprint arXiv:1611.01144*, 2016.

[62] A. Gersho, R. M. Gray. Vector quantization and signal compression. *Springer Science & Business Media*, 2012.

[63] A. Vasuki, P. T. Vanathi. A review of vector quantization techniques. *IEEE Potentials*, 2006, 25(4): 39-47.

[64] S. Black, S. Biderman, E. Hallahan, et al. Gpt-neox-20b: An open-source autoregressive language model. *arXiv preprint arXiv:2204.06745*, 2022.

[65] H. Touvron, T. Lavigl, G. Izacard, et al. Llama: Open and efficient foundation language models. *arXiv preprint arXiv:2302.13971*, 2023.

[66] S. Narang, A. Chowdhery. Pathways language model (palm): Scaling to 540 billion parameters for breakthrough performance. *Google AI Blog*, 2022.

[67] Y. Li, Y. Song, J. Luo. Improving pairwise ranking for multi-label image classification. In *Proceedings of the IEEE Conference on Computer Vision and Pattern Recognition*, 2017, pp. 3617-3625.

[68] Y. Sun, C. Cheng, Y. Zhang, et al. Circle loss: A unified perspective of pair similarity optimization. In *Proceedings of the IEEE/CVF Conference on Computer Vision and Pattern Recognition*, 2020, pp. 6398-6407.